Available online at www.sciencedirect.com
SCIENCE DIRECT®
Phytochemistry 66 (2005) 1465–1471
PHYTOCHEMISTRY
www.elsevier.com/locate/phytochem

Tagalsins A–H, dolabrane-type diterpenes from the mangrove plant, *Ceriops tagal*

Yan Zhang [a,c], Zhiwei Deng [b], Tianxiang Gao [c], Peter Proksch [d], Wenhan Lin [a,*]

[a] *State Key Laboratory of Natural and Biomimetic Drugs, Peking University, Beijing 100083, People's Republic of China*
[b] *Analytical and Testing Center, Beijing Normal University, Beijing 100073, People's Republic of China*
[c] *Ocean University of China, Qingdao 266003, People's Republic of China*
[d] *Institute of Pharmaceutical Biology, Heinrich-Heine-University Duesseldorf, D-40225 Duesseldorf, Germany*

Received 12 November 2004; received in revised form 15 February 2005
Available online 31 May 2005

Abstract

From the stems and twigs of the mangrove plant, *Ceriops tagal*, seven dolabrane-type diterpenes, namely tagalsins A–G (**1**–**7**), and the norditerpene tagalsin H (**8**) were isolated. Their structures were established on the basis of extensive spectroscopic analysis.

Keywords: *Ceriops tagal*; Mangrove; Diterpenes; Tagalsins A–H; Structure elucidation

1. Introduction

Mangrove plants of the genus *Ceriops* (Rhizophoraceae), represented by two species, *C. decandra* and *C. tagal*, are widely distributed along the sea coasts of Africa, South Asia and South Pacific islands (Anjaneyulu and Rao, 2002; Shukla and Chandel, 1991). These plants are used as a folk remedy, e.g., against sores (Lin and Fu, 1995). The decoction of the bark of *C. tagal* was used to treat haemorrhages and malignant ulcers in India (Rastogi and Mehrotra, 1991), while the water and alkaline extracts from the leaves of *C. decandra* were shown to posses radical modulation activity in scavenging superoxide anions produced by hypoxanthin–xanthine oxidase (Anjaneyulu and Rao, 2002). Both of the plants are a rich source of tannins and triterpenoids (Ghosh et al., 1985). Previous chemical examination on *C. decandra* yielded a number of kaurene and gibberellin-type diterpenoids, (Ghosh et al., 1985; Anjaneyulu et al., 2002; Anjaneyulu and Rao, 2002, 2003), but *C. tagal* has not been investigated phytochemically. In continuation of our studies on Chinese mangrove plants, we examined *C. tagal* (Perr.) collected in the mangrove forest in Hainan Island. Repeated column chromatography of the EtOH extract led to the isolation and characterization of seven new dolabrane-type diterpenes (**1**–**7**) and a new norditerpene (**8**). Their structures were determined by extensive spectroscopic data analysis.

2. Results and discussion

Tagalsin A (**1**) was obtained as pale yellow crystals and its molecular formula was determined as $C_{20}H_{28}O_3$ by HRFABMS, which was in agreement with the ^1H and ^{13}C NMR spectra. The IR absorptions at 3409 and 1672 cm^{-1} suggested the presence of hydroxyl substituents and of an enone group. The ^1H NMR spectrum exhibited three angular methyls at δ 0.77 (*s*, H_3-20), 1.05 (*s*, H_3-17), and 1.18 (*s*, H_3-19), an olefinic

* Corresponding author. Tel.: +86 10 620 62210; fax: +86 10 828 02724.
E-mail address: whlin@bjmu.edu.cn (W. Lin).

0031-9422/$ - see front matter © 2005 Elsevier Ltd. All rights reserved.
doi:10.1016/j.phytochem.2005.04.018

proton at δ 6.34 (*d*, J = 6.8 Hz, H-1), and a terminal vinylic group at δ 5.79 (*dd*, J = 17.5, 10.7 Hz, H-15), 4.92 (brd, J = 17.5 Hz, H-16a), and 4.85 (brd, J = 10.7 Hz, H-16b), along with a pair of isolated epoxidic geminal signals at δ 2.96 (d, J = 6.1 Hz, H-18a) and 3.44 (*d*, J = 6.1 Hz, H-18b). The ^{13}C NMR and DEPT spectra displayed twenty carbons involving four olefinic carbons at δ 120.6 (*d*, C-1), 147.7 (*s*, C-2), 150.8 (*d*, C-15) and 108.9 (*t*, C-16), and an enone carbonyl carbon at δ 191.2 (*s*, C-3). The NMR spectroscopic features (Tables 1 and 2) were characteristic of a dolabrane-type diterpene (Fig. 1), closely related to oxidopanamensin, whose structure was determined by X-ray diffraction (Koike et al., 1980). In the DQFCOSY spectrum, the olefinic proton H-1 showed a correlation with H-10 (δ 2.14, d, J = 6.8 Hz), indicating the vinyl carbons of an enone unit located at C-1 and C-2 of ring A. A D_2O exchangeable broaden signal at δ 6.15 (br) was attributable to a hydroxyl group at C-2, which was considered to form a hydrogen-bond with the oxo group at C-3 due to the pronounced lowfield chemical shift. This finding could explain the stable enol group at ring A of **1** and also occurred latter in tagalsins B (**2**) and C (**3**) and tagalsin G (**7**). The HMBC correlations of the epoxidic protons to C-4 (δ 60.1, *s*), C-3 and C-5 (δ 35.6, *s*), H-10 to C-2, C-19 (δ 31.6, *q*), and C-20 (δ 12.1, *q*), along with H-1 to C-3, C-5 (δ 35.6, *s*) and C-9 (δ 39.7, *s*) (Fig. 2), confirmed the substructure in ring A to be the same as that found in oxidopanamensin. Further HMBC correlations from H_3-19 to C-4, C-5, C-10, and C-6 (δ 34.2, *t*) indicated a methylene at C-6 in **1** instead of a hydroxylated methine as in oxidopanamensin. The relative stereochemistry was assigned mainly by analysis of the NOESY spectrum. The presence of NOE correlations between H-10/H_3-19, H-10/H-8 and H-8/H_3-17 and the absence of NOE correlation between H_3-20/H-8 allowed the assignment of the ring conjunction as *cis*-form for A/B and *trans*-form for B/C, and a β-orientation for Me-17, the same as reported for oxidopanamensin. The similar optical rotation of **1** ($[\alpha]_D$ + 69.26°) and of oxidopanamensin-2,6-diacetate ($[\alpha]_D$ + 79°) (Koike et al., 1980) was also in agreement with the identical geometry of the tricyclic ring. However, the ^{1}H signals of H_3-19 and H_2-18 (Table 2) in **1** showed remarkable differences from those of oxidopanamensin [δ 1.28 (*s*, H_3-19), 3.12 (*s*, H_2-18)], implying a different configuration of the epoxidic group at C-4 in both compounds. The observed NOE correlation between δ 2.96 (*d*, H-18a) and δ 1.44 (*m*, H-6α) and the absence of a NOE correlation between H_2-18/H_3-19 clarified the orientation of the epoxidic methylene opposite to H_3-19 (see Fig. 2).

Analysis of the ^{1}H and ^{13}C NMR spectra (Tables 1 and 2) and comparison of the NMR spectroscopic data with those of **1** indicated that tagalsin B–H (**2**–**8**) shared the same partial structures for rings B and C as for **1**, but differed solely in the substructure of ring A.

The molecular formula of tagalsin B (**2**) was identical to that of **1** as indicated by HRFABMS. The ^{1}H and ^{13}C NMR spectroscopic data of **2** were also comparable with those of 1, with exception of the signals for the epoxidic group at C-4 in **2** that were shifted to δ 3.13 (1H, *d*, J = 6.2 Hz, H-18a) and 3.10 (1H, *d*, J = 6.2 Hz, H-18b), and the ^{13}C chemical shift of C-18 which resonated at δ 55.5 (*t*) in **2** contrast with δ 50.6 (*t*, C-18) in **1**. This evidence suggested that **2** was an isomer of **1**

Table 1
^{13}C NMR spectroscopic data of tagalsins A–H (**1**–**8**)[a]

C	1	2	3	4	5	6	7	8
1	120.6 *d*	119.0 *d*	118.2 *d*	15.7 *t*	18.0 *t*	16.1 *t*	33.2 *t*	31.1 *t*
2	147.7 s	147.2 s	147.2 *s*	29.1 *t*	36.7 *t*	31.5 *t*	193.1 *s*	179.5 *s*
3	191.2 *s*	191.9 *s*	185.3 *s*	73.4 *d*	203.7 *s*	199.6 *s*	144.5 *s*	
4	60.1 *s*	61.1 *s*	148.8 *s*	62.3 *s*	152.5 *s*	116.7 *s*	135.5 *s*	214.7 *s*
5	35.6 *s*	36.9 *s*	41.2 *s*	35.9 *s*	41.2 *s*	36.3 *s*	39.0 *s*	50.4 *s*
6	34.2 *t*	32.0 *t*	36.6 *t*	34.4 *t*	37.6 *t*	36.7 *t*	38.0 *t*	38.7 *t*
7	27.2 *t*	27.1 *t*	25.4 *t*	27.9 *t*	25.8 *t*	25.5 *t*	26.7 *t*	27.3 *t*
8	40.8 *d*	40.0 *d*	40.8 *d*	41.8 *d*	42.7 *d*	42.5 *d*	41.6 *d*	42.1 *d*
9	39.7 *s*	39.1 *s*	40.8 *s*	37.4 *s*	38.4 *s*	37.7 *s*	38.1 *s*	38.6 *s*
10	54.3 *d*	54.7 *d*	55.5 *d*	54.7 *d*	52.6 *d*	51.8 *d*	54.5 *d*	54.3 *d*
11	35.0 *t*	34.6 *t*	35.2 *t*	35.9 *t*	35.8 *t*	35.2 *t*	34.2 *t*	33.0 *t*
12	31.7 *t*	31.5 *t*	31.6 *t*	32.1 *t*	32.1 *t*	31.7 *t*	31.7 *t*	31.8 *t*
13	36.4 *s*	36.1 *s*	36.5 *s*	36.2 *s*	36.6 *s*	36.1 *s*	36.2 *s*	36.2 *s*
14	39.4 *t*	39.2 *t*	39.4 *t*	38.9 *t*	39.2 *t*	38.8 *t*	38.9 *t*	39.1 *t*
15	150.8 *d*	150.4 *d*	150.8 *d*	151.2 *d*	151.2 *d*	150.9 *d*	150.9 *d*	150.9 *d*
16	108.9 *t*	108.9 *t*	108.9 *t*	108.8 *t*	109.1 *t*	108.8 *t*	108.9 *t*	108.9 *t*
17	22.9 *q*	22.6 *q*	22.9 *q*	22.8 *q*	23.2 *q*	23.0 *q*	23.1 *q*	23.1 *q*
18	50.6 *t*	55.5 *t*	118.9 *t*	56.5 *t*	116.5 *t*	171.2 *d*	11.6 *q*	27.6 *q*
19	31.6 *q*	29.2 *q*	33.9 *q*	30.8 *q*	33.8 *q*	35.8 *q*	31.6 *q*	28.4 *q*
20	12.1 *q*	12.9 *q*	12.0 *q*	16.8 *q*	13.9 *q*	12.7 *q*	13.7 *q*	12.3 *q*

[a] Chemical shifts in δ from TMS (multiplicity, J in Hz) in $CDCl_3$.

Table 2
^{1}H NMR spectroscopic data of tagalsins A–H (**1**–**8**)[a]

H	**1**	**2**	**3**	**4**	**5**	**6**	**7**	**8**
1	6.34 *d* (6.8)	6.30 *d* (6.7)	6.22 *d* (6.7)	1.82 *m*	2.00 *m*	1.97 *m*	2.77 *d* (18.7)	2.66 *dd* (7.0, 18.0)
				2.04 *ddd* (4.0, 4.5, 14.0)	2.11 *m*	2.04 *ddd* (7.0, 9.0, 16.5)	2.87 *dd* (6.5, 18.7)	3.15 *dd* (2.0, 18.0)
2				1.80 *m*	2.53 *dd* (8.5, 13.5)	2.46 *dd* (3.0, 13.0)		
				2.15 *m*	2.54 *dd* (5.0, 13.5)	2.45 *dd* (9.0, 13.0)		
3				3.45 *dd* (1.5, 2.0)				
6	1.19 *m*	1.18 *m*	1.48 *m*	0.98*m*	1.48 *ddd* (2.5, 14.0, 15.0)	1.42 *ddd* (4.0, 13.0, 14.0)	1.30 *m*	1.31 *m*
	1.44 *m*	1.60 *m*	2.20 *ddd* (2.5, 2.5, 14.5)	1.59 *ddd* (2.5, 3.0, 14.5)	2.15 *m*	2.13 *ddd* (4.0, 3.0, 14.0)	2.19 *ddd* (2.5, 2.5, 13.5)	2.32 *ddd* (2.5, 2.5, 14.0)
7	1.06 *m*	1.18 *m*	1.20 *m*	0.99 *m*	1.12 *m*	1.10 *m*	1.18 *m*	1.20 *m*
	1.48 *m*	1.22 *m*	1.32 *m*	1.08 *m*	1.32 *m*	1.23 *m*	1.53 *m*	1.46 *m*
8	1.40 *m*	1.45 *m*	1.46 *m*	1.33 *m*	1.40 *ddd* (2.0, 2.0, 11.5)	1.41 *ddd* (1.5, 13.0, 13.5)	1.41 *m*	1.52 *m*
10	2.14 *d* (6.8)	2.21 *d* (6.7)	2.08 *d* (6.7)	1.39 *m*	1.34 *m*	1.24 *m*	1.68 *d* (6.5)	1.89 *dd* (2.0, 7.0)
11	1.40 *dd* (10.5, 12.5)	1.42 *m*	1.34 *m*	1.18 *ddd* (4.0, 13.5, 13.5)	1.12 *m*	1.10 *ddd* (3.5, 13.0, 14.0)	1.12 *ddd* (4.0, 13.5, 13.5)	1.30 *m*
	1.52 *ddd* (3.0, 4.0, 12.5)	1.55 *m*	1.53 *m*	1.78 *m*	1.69 *ddd* (3.5, 3.5, 13.0)	1.62 *ddd* (3.0, 4.0, 13.0)	1.66 *ddd* (3.5, 3.5, 13.5)	1.51 *m*
12	1.20 *dd* (3.0, 14.0)	1.25 *m*	1.20 *m*	1.25 *m*	1.22 *ddd* (3.0, 3.5, 13.0)	1.20 *ddd* (3.0, 3.5, 14.0)	1.21 *ddd* (3.5, 4.0, 13.5)	1.22 *m*
	1.48 *dd* (4.0, 10.5, 14.0)	1.45 *m*	1.48 *m*	1.47 *ddd* (4.0, 13.5, 13.5)	1.52 *ddd* (3.5, 13.0, 13.0)	1.53 *ddd* (4.0, 14.0, 14.0)	1.54 *ddd* (4.0, 13.5, 13.5)	1.52 *m*
14	1.03 *m*	1.11 *dd* (3.0, 13.5)	1.10 *m*	0.98 *m*	0.98 *m*	0.96 *ddd* (1.5, 1.5, 13.5)	1.02 *m*	1.00 *m*
	1.34 *dd* (11.5, 12.5)	1.33 *dd* (13.0, 13.5)	1.30 *m*	1.32 *dd* (12.0, 13.0)	1.30 *m*	1.32 *dd* (13.0, 13.5)	1.40 *dd* (13.0, 13.5)	1.38 *m*
15	5.79 *dd* (10.7, 17.5)	5.88 *dd* (17.5, 10.8)	5.80 *dd* (17.5, 10.8)	5.80 *dd* (17.5, 10.8)	5.79 *dd* (17.5, 10.8)	5.78 *dd* (17.5, 10.7)	5.81 *dd* (17.5, 10.8)	5.78 *dd* (17.5, 10.5)
16	4.85 *brd* (10.7)	4.86 *d* (10.8)	4.87 *d* (10.8)	4.84 *d* (10.8)	4.92 *d* (17.5)	4.88 *d* (17.5)	4.94 *d* (17.5)	4.88 *d* (17.5)
	4.92 *brd* (17.5)	4.91 *d* (17.5)	4.90 *d* (17.5)	4.90 *d* (17.5)	4.84 *d* (10.8)	4.84 *d* (10.7)	4.87 *d* (10.8)	4.84 *d* (10.5)
17	1.05 *s*	1.06 *s*	1.05 *s*	1.01 *s*	1.02 *s*	1.01 *s*	1.05 *s*	1.04 *s*
18	2.96 *d* (6.1)	3.11 *d* (6.2)	5.43 *brs*	2.70 *d* (4.6)	5.92 *brs*	7.90 *d* (7.8)	1.90 *s*	2.22 *s*
	3.44 *d* (6.1)	3.13 *d* (6.2)	6.26 *brs*	3.08 *d* (4.6)	5.24 *brs*			
19	1.18 *s*	1.21 *s*	1.14 *s*	1.39 *s*	1.08 *s*	1.15 *s*	1.27 *s*	1.17 *s*
20	0.77 *s*	0.73 *s*	0.64 *s*	0.87 *s*	0.78 *s*	0.69 *s*	0.62 *s*	0.58 *s*

[a] Measured at 500 MHz (the chemical shifts of the respective protons at highfield were taken from HMQC data and the part of the multiplicities not resolved). Chemical shifts in δ from TMS (multiplicity, J in Hz) in $CDCl_3$.

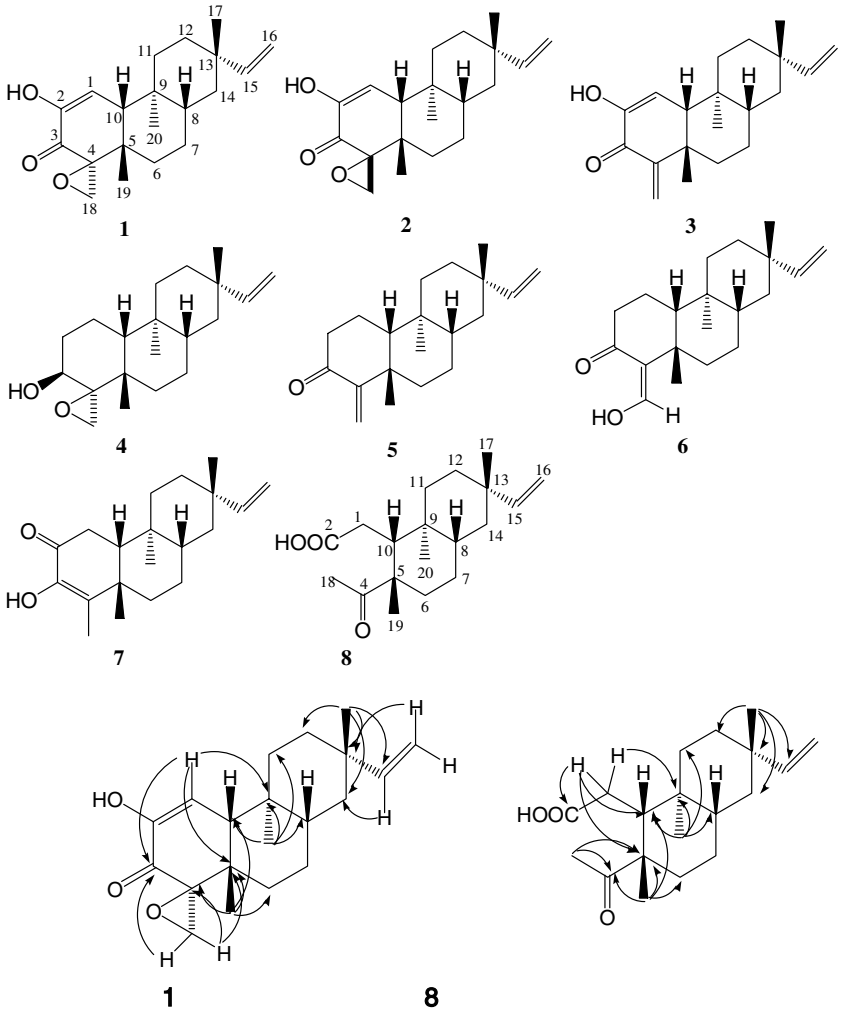

Fig. 1. Main HMBC correlations of **1** and **8**.

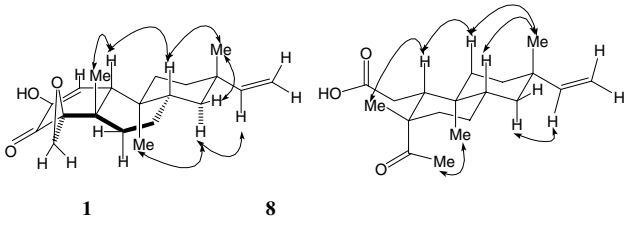

Fig. 2. Key NOE correlations of **1** and **8**.

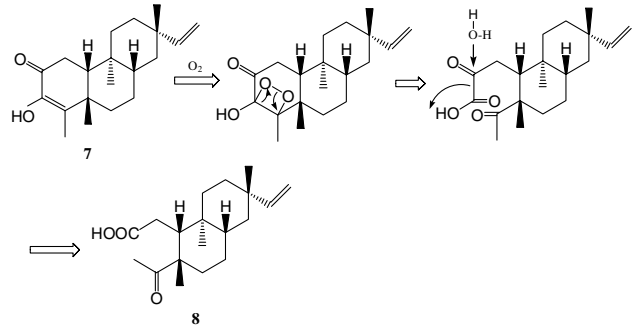

Fig. 3. Proposed transformation from **7** to **8**.

differing in configuration at C-4. The observation of the NOESY correlation between H_2-18/H-19 δ 1.21 (3H, *s*), and the similarity of the remaining NOE correlations when compared to those of **1**, confirmed the structure of **2** to be an epimer of **1** at C-4.

The molecular weight of tagalsin C (**3**) was 16 mass units smaller than that of tagalsin A (**1**), suggesting the loss of one oxygen atom, which was confirmed by HRFABMS. Comparison of IR, ^{1}H and ^{13}C NMR spectroscopic data of both compounds revealed that signals assigned to rings B and C were very similar, while the resonances assigned to ring A were almost identical to those of ent-5α,3,15-dioxodobr-1,4(18)-diene-2,16-diol (Kijjoa et al., 1994), where the extra-methylene [δ 5.43 (1H, br, H-18a), 6.26 (1H, br, H-18b), 118.9 (*t*, C-18)] of **2** replaced the epoxidic group of 1. The HMBC correlations of H_2-18 with C-3 (δ 185.3, *s*), C-5 (δ 41.2, *s*), and C-4 (δ 148.8, *s*) confirmed the assignment of the respective substructure in ring A. The relative stereochemistry of **3** was determined to be the same as that

of **1** based on NOE correlations between H_3-19/H-8, H_3-19/H-10, H-18a/H-6α(δ 2.20), and H-8/H_3-17, in association with the comparable NMR data detected for both compounds.

The ^1H and ^{13}C NMR spectra of tagalsin D (**4**) were consistent with the molecular formula $C_{20}H_{32}O_2$, which was further confirmed by HRFABMS. The IR absorptions at 3406 and 1635 cm^{-1} suggested the presence of hydroxyl and vinyl groups. Comparison of the ^1H and ^{13}C NMR spectroscopic data (Tables 1 and 2) indicated that **4** contained the same 13-vinyl substituted dolabrane backbone as in tagalsin A, while significant differences in the ^{13}C NMR spectrum were attributable to ring A where a hydroxylated methine (δ 73.4, *d*, C-3) and two methylenes [δ 15.7 (*t*, C-1), 29.1 (t, C-2)] were observed for **4** instead of enone signals as in **1**. The epoxide group at C-4 of **1** was still present in **4** due to the NMR signals at δ 2.70 (1H, *d*, $J = 4.6$ Hz, H-18a), 3.08 (1H, *d*, $J = 4.6$ Hz, H-18b) and 56.5 (*t*, C-18) and 62.3 (*s*, C-4). The HMBC correlations between H_2-18 and carbons at C-4, C-3 and C-5 (δ 35.9, s) deduced the attachment of a hydroxyl group at C-3. The spin coupling of H-3 (δ 3.45, dd, $J = 2.0$, 1.5 Hz) suggested that it is an equatorial proton (α-orientation), and the presence of NOE correlations between H-3 and H-18a and the absence of NOE correlations between H_2-18 and H_3-19 (δ 1.39, *s*) confirmed the configuration of the epoxide group at C-4 to be the same as found for **1**. A pronounced downfield shift of NMR signals for H_3-20 (δ 0.83, *s*) and C-20 (δ 16.8, *q*) (when compared to the spectra of the other tagalsins) could be explained by the deshielding methyl group induced by epoxidic group through their close spatial relationship when the cyclohexane ring A was in a stable chair-form.

The molecular formula of tagalsin E (**5**) was determined as $C_{20}H_{30}O$ on the basis of HRFABMS. Inspection of the ^1H and ^{13}C NMR spectroscopic data of **5** (Tables 1 and 2) revealed that the signals assigned to rings B and C were very similar with those obtained for **3**. However, the enone signals observed in **3** were replaced by a ketone group at δ 203.7 (*s*, C-3) of **5**. The olefinic protons at δ 5.24 (1H, br, H-18a) and 5.92 (1H, br, H-18b) and their directly connected carbon at δ 116.5 (*t*, C-18) were attributable to an olefinic methylene group at C-4, which was further supported by the HMBC correlations of H_2-18 with the carbons at δ 41.2 (*s*, C-5) and 203.7 (*s*).

The molecular formula of tagalsin F (**6**) was $C_{20}H_{30}O_2$ as indicated by HRFABMS. Tagalsin F thus differed from **5** by an additional oxygen atom. The ^1H and ^{13}C NMR spectra of **6** were very similar to those of **5** with the exception of the signals for ring A, where an olefinic proton at δ 7.90 (1H, *d*, $J = 7.8$ Hz, H-18) was observed to correlate with a D_2O exchangeable proton at δ 15.46 (1H, *d*, $J = 7.8$ Hz) in DQFCOSY spectrum instead of ex-methylene protons as in **5**. In addition, the signal of C-18 (δ 171.2, *d*) suffered a large downfield shift which was indicative for a hydroxyl group attached at C-18. The marked downfield chemical shift of OH-18 suggested the formation of a strong hydrogen bond with a ketone. Thus, the configuration of the double bond at C-4 was assigned as having Z-geometry.

The molecular formula of tagalsin G (**7**) was the same as that of **6**, as determined by HRFABMS. The IR absorptions at 3429, 1667, and 1640 cm^{-1} suggested the presence of hydroxyl substituents and of an enone group. Comparison of the NMR spectroscopic data (Tables 1 and 2) of **7** with those of ent-5α,2,15-dioxodolabr-3-ene-3, 16-diol (Kijjoa et al., 1994) and those of tagalsin A–F indicated that ring A was a 3-hydroxy-4-methyl-2-enone cyclohexane and the partial structures of rings B and C were identical to those of tagalsin A–F. The stereochemistry of **7** was regarded to be the same as that of **6** on the basis of similar NOE correlations and comparable NMR data.

Tagalsin H (**8**) showed nineteen carbons in ^{13}C NMR spectrum, and its molecular formula was determined as $C_{19}H_{30}O_3$ by HRFABMS. The IR absorptions at 1711 and 1635 cm^{-1} suggested the presence of carbonyl and vinyl groups. The ^1H NMR spectrum displayed four methyl groups at δ 0.58 (3H, *s*, H-18), 1.04 (3H, *s*, H-17), 1.17 (3H, *s*, H-19), and 2.22 (3H, *s*, H-3), and the terminal vinylic protons in tagalsins A-G were also observed in **8** resonating at δ 5.78 (1H, *dd*, $J = 17.5$, 10.5 Hz, H-15), 4.88 (1H, brd, $J = 17.5$ Hz, H-16a), 4.84 (1H, brd, $J = 10.5$ Hz, H-16b). A detailed 2D NMR (HMQC, HMBC and COSY) investigation revealed that rings B and C were identical to those of **1**–**7**, but the spectroscopic evidence indicated that C-3 was excised, C-2 had become a carboxyl carbon (δ 179.5, *s*), and C-5 was attached to a methyl ketone [δ 2.22 (*s*, H_3-18), 27.6 (*q*, C-18), 214.7 (*s*, C-4)], as found for ent-2-seco-3-nor-5α,4,15-dioxo-16-hydroxydolabran-2-oic acid (Kijjoa et al., 1994). The NOESY correlations between H_3-19/H-10, H-1a/H_3-18, H-10/H-8 (δ 1.52, *m*), and H-8/H_3-17 suggested the relative stereochemistry at rings B and C as found for **1**. A partial conversion of **7** to **8** by air oxidation proved that the stereochemistries of both compounds were identical. It is interesting to note that ent-2-seco-3-nor-5α,4,15-dioxo-16- hydroxydolabran-2-oic acid and related compounds were also obtained from 2-oxo-3-hydroxy-3-ene-dolabranes by air oxidation (Kijjoa et al., 1994, 1995). We postulate a possible mechanism for the oxidative fragmentation, in which a peroxycyclization occurs at the C3=C4 thereby generating a dioxetane intermediate that fragments to yield a ketone at C-4 and a carboxyl group at C-3. The carboxyl group is lost as carbon dioxide to form an aldehyde group at C-2 which could easily be further oxidized to produce a carboxyl substituent (see Fig. 3).

Dolabrane-type diterpenoids are a small group of natural products reported mainly from the plant genera *Thujopsis*, *Erythroxylonpictum*, *Rondeletia* (Koike et al., 1980), and from the liverwort *Schistochila aligera* (Nagashima et al., 1991). This is a first report of dolabranes from marine mangrove plants. The constituents of *C. tagal* are quite different to those of *C. decandra* which mainly produced kaurene-type diterpenoids and derivatives, implying that both species generate secondary metabolites through different metabolic pathways. This evidence is helpful for the chemotaxonomy of mangrove plants.

Tagalsins A–H (**1**–**8**) were tested for their in vitro cytotoxicity against cultured human tumor cell lines HL-60, Bel-7402, and Hela, but showed no activity at the range of concentrations used.

3. Experimental

3.1. General

Melting points were measured on a XT-4A micro-melting point apparatus without correction. IR spectra were determined on a Thermo Nicolet Nexus 470 FT-IR spectrometer. NMR spectra were recorded on a Bruker Avance-500 FT NMR spectrometer using TMS as internal standard. EIMS was performed with a Bruker APEX II mass spectrometer, and HRFABMS spectra were recorded on a Bruker FT-ICRMS spectrometer. Column chromatography was carried out on silica gel (200–300 mesh), and HF_{254} silica gel for TLC was obtained from Qingdao Marine Chemistry Co. Ltd.. Qingdao. People's Republic of China. Sephadex LH-20 (18–110 μm) was obtained from Pharmacia.

3.2. Plant material

The specimen of *Ceriops tagal* was collected at the mangrove garden in Hainan Island, People's Republic of China, in July 2002. The species was identified by Prof. Lin Peng of Xiamen University. A voucher specimen (HN-032) was deposited at the State Key Laboratory of Natural and Biomimetic Drugs, Peking University.

3.3. Extraction and isolation

The stems and twigs of *C. tagal* (3.3 kg) were air-dried and then ground. The powdered sample was percolated with 95% EtOH twice at room temperature, and the EtOH extract was concentrated in vacuum to afford a black residue. This residue was partitioned between H_2O and petrol, EtOAc, and *n*-BuOH, successively. The petrol extract (19 g) was subjected to silica gel cc and eluted with petrol–EtOAc as a gradient to obtain ten fractions. Fraction A (0.5 g, 20:1) was applied to a silica gel column eluted with petrol–Et_2O (15:1) to obtain tagalsin F (**6**) (128 mg). Fraction C (0.6 g, 15:1) was subjected to a Sephadex LH-20 column and eluted with $CHCl_3$–MeOH (1:1) to yield tagalsins E (**5**) (15.6 mg), C (**3**) (16.6 mg), G (**7**) (10.5 mg) and H (**8**) (10.0 mg). Fraction E (60 mg, 10:1) was subjected to silica gel cc and eluted with petrol–acetone (8:1) to afford tagalsins A (**1**) (15.6 mg), B (**2**) (17.5 mg), and D (**4**) (11.2 mg). Tagalsin A (**1**) was recrystallized as needles from acetone.

Tagalsin G (**7**) was partially converted to tagalsin H (**8**) when exposed to air for approximately one week.

3.4. Tagalsin A (*1*)

Pale yellow needle crystals. m.p. 67–69 °C; $[\alpha]_D^{25} + 69.26^\circ$ (c0.054, $CHCl_3$); IR (KBr) ν_{max} 3409, 2926, 2859, 1672, 1457, 1412, 1005 cm^{-1}; For ^1H and ^{13}C NMR spectroscopic data, see Tables 1 and 2; EIMS *m/z* 316 $[M]^+$ (15), 286 (17), 259 (20), 179 (27), 163 (53), 136 (100), 107 (93); HRFABMS *m/z* 317.21110 $[M + H]^+$ (calcd for $C_{20}H_{29}O_3$, 317.21111).

3.5. Tagalsin B (*2*)

White solid. m.p. 66–68 °C; $[\alpha]_D^{25} + 165^\circ$ (c0.06, $CHCl_3$); IR (KBr)ν_{max} 3430, 2922, 2853, 1681, 1636, 1599, 1515, 1462, 1412, 1219, 1009 cm^{-1}; For ^1H and ^3C NMR spectroscopic data, see Tables 1 and 2; EIMS *m/z* 316 $[M]^+$ (17), 283 (20), 255 (18), 175 (49), 136 (63), 107 (100), 81 (69), 67 (43), 55 (50); HRFABMS *m/z* 317.2110 $[M + H]^+$ (calcd for $C_{20}H_{29}O_3$, 317.2111).

3.6. Tagalsin C (*3*)

Yellow oil. $[\alpha]_D^{25} + 92.3^\circ$ (c0.05, $CHCl_3$); IR (KBr)ν_{max} 3403, 3082, 2924, 2859, 1662, 1605, 1459, 1411, 1220, 1082 cm^{-1}; For ^1H and ^{13}C NMR spectroscopic data, see Tables 1 and 2; EIMS *m/z* 300 $[M]^+$ (26), 163 (35), 151 (45), 138 (77), 107 (100), 93 (60), 79 (77); HRFABMS *m/z* 301.2162 $[M + H]^+$ (calcd for $C_{20}H_{29}O_2$, 301.2162).

3.7. Tagalsin D (*4*)

White solid. m.p. 64–66 °C; $[\alpha]_D^{25} + 38.4^\circ$ (c0.074, $CHCl_3$); IR (KBr)ν_{max} 3406, 3059, 2924, 2860, 1635, 1476, 1450, 1373, 1264, 943 cm^{-1}; For ^1H and ^{13}C NMR spectroscopic data, see Tables 1 and 2; EIMS *m/z* 304 $[M]^+$ (5), 289 (12), 274 (33), 259 (26), 241 (34), 189 (25), 147 (32), 133 (46), 121 (51),107 (98); HRFABMS *m/z* 305.2474 $[M + H]^+$ (calcd for $C_{20}H_{33}O_2$, 305.2475).

3.8. Tagalsin E (5)

Yellow solid. m.p. 73–75 °C; $[\alpha]_D^{25} + 7.85°$ (*c*0.07, $CHCl_3$); IR (KBr)ν_{max} 2956, 2923, 2860, 1692, 1636, 1607, 1457, 1377, 908 cm^{-1}; For ^1H and ^{13}C NMR spectroscopic data, see Table 1 and 2; EIMS *m/z* 286 $[M]^+$ (24), 271 (22), 243 (22), 202 (30), 189 (25), 161 (27), 149 (66), 121 (70),107 (100), 93 (88), 79 (85); HRFABMS *m/z* 287.2368 $[M + H]^+$ (calcd for $C_{20}H_{31}O$, 287.2369).

3.9. Tagalsin F (6)

White solid. m.p. 98–99 °C; $[\alpha]_D^{25} + 34.86°$ (*c*0.072, $CHCl_3$); IR (KBr) ν_{max} 3084, 2967, 2922, 2857, 1622, 1455, 1384, 1188 cm^{-1}; For ^1H and ^{13}C NMR spectroscopic data, see Tables 1 and 2; FABMS *m/z* 303 $[M + H]^+$; HRFABMS *m/z* 303.2319 $[M + H]^+$ (calcd for $C_{20}H_{31}O_2$, 303.2318).

3.10. Tagalsin G (7)

Colorless oil; $[\alpha]_D^{25} + 55.97°$ (*c*0.09, $CHCl_3$); IR (KBr) ν_{max} 3429, 2924, 2857, 1732, 1667, 1640, 1451, 1394, 1201, 1101 cm^{-1}; For ^1H and ^{13}C NMR spectroscopic data, see Tables 1 and 2. EIMS *m/z* 302 $[M]^+$ (8), 287 (43), 263 (53), 203 (100), 149 (73), 107 (89), 93 (55), 81 (56); HRFABMS *m/z* 303.2319 $[M + H]^+$ (calcd for $C_{20}H_{31}O_2$, 303.2318).

3.11. Tagalsin H (8)

White powder. m.p. 101–102 °C; IR (KBr)ν_{max} 3077 (br), 2971, 2926, 2870, 1711, 1636, 1465, 1412, 1214, 908 cm^{-1}; For ^1H and ^{13}C NMR spectroscopic data, see Tables 1 and 2. Negative HRFABMS *m/z* 305.2120 $[M - H]^-$ (calcd for $C_{19}H_{29}O_3$, 305.2122).

Acknowledgements

This study was supported by grants from the National High Technology Development Project (863 project) (Nos. 2001AA620403 and 2002AA217081), NSFC (Nos. 40176038 and 30171106), and from the International Cooperation Projects of BMBF-CNCBD. We thank Prof. P. Lin of Xia Men University (People's Republic of China) for identification of the plant material.

References

Anjaneyulu, A.S.R., Rao, V.L., Lobkovsky, E., Clardy, J., 2002. Ceripsin E, a new epoxy *ent*-kaurene diterpenoid from *Ceriops decandra*. J. Nat. Prod. 65, 592–594.

Anjaneyulu, A.S.R., Rao, V.L., 2002. Ceripsins A–D, diterpenoids from *Ceriops decandra*. Phytochemistry 60, 777–782.

Anjaneyulu, A.S.R., Rao, V.L., 2003. Ceripsins F and G, diterpenoids from *Ceriops decandra*. Phytochemistry 62, 1207–1211.

Ghosh, A., Misra, S., Dutta, A.K., Choudhury, A., 1985. Pentacyclic triterpenoids and sterols from seven species of Mangrove. Phytochemistry 24, 1725–1727.

Kijjoa, A., Polonia, M.A., Pinto, M.M.M., Kitiratakarn, T., Gedris, T.E., Herz, W., 1994. Dolabranes from Endospermun diadenum. Phytochemistry 37, 197–200.

Kijjoa, A., Pinto, M.M.M., Anantachoke, C., Gedris, T.E., Herz, W., 1995. Dolabranes from Endospermun diadenum. Phytochemistry 40, 191–193.

Koike, K., Cordell, G.A., Farnsworth, N.R., 1980. New cytotoxic diterpenes from *Rondeletia panamensis* (Rubiaceae). Tetrahedron 36, 1167–1172.

Lin, P., Fu, Q., 1995. Environmental Ecology and Economic Utilization of Mangroves in China. Higher Education Press, Beijing, pp. 1–95.

Nagashima, F., Tori, M., Asakawa, Y., 1991. Diterpenoids from the east Malaysian liverwort *Schistochila aligera*. Phytochemistry 30, 849–851.

Rastogi, R.P., Mehrotra, B.N., 1991. Compendium of Indian Medicinal Plants, vol. 1. Publications & Information Directorate, New Delhi.

Shukla, R.S., Chandel, P.S., 1991. Plant Ecology and Soil Science. S. Chand and Company Ltd., New Delhi.